Emergence of heterogeneous structures in chemical reaction-diffusion networks

Qi Xuan*
Department of Automation, Zhejiang University of Technology, Hangzhou 310023, China

Fang Du and Tie-Jun Wu
Department of Control Science and Engineering, Zhejiang University, Hangzhou 310027, China

Guanrong Chen
Department of Electronic Engineering, City University of Hong Kong, Hong Kong, China

(Received 8 June 2010; revised manuscript received 14 September 2010; published 25 October 2010)

This paper suggests that reaction-diffusion processes, rather than pure topological rules, are responsible for the emergence of heterogeneous structures of complex chemical reaction networks. In such a network, chemical substances react in each node and diffuse between connected nodes. At the same time, each node is able to sense the difference between its own state and the environmental conditions and can rearrange its neighbors via a local rewiring process so as to eliminate the sensed difference. Then, the network, even originally homogeneous, will develop a heterogeneous structure under certain environmental conditions. Such a resultant heterogeneous network may be disassortative, highly clustering, and small world as well. This implies that the reaction-diffusion equilibrium can be statistically controlled by slightly changing the structure of the underlying network. This structure-control mechanism may be especially useful in the situations where some other macroscopic measurements, such as temperature and pressure, are not allowed to be changed through the process.

DOI: 10.1103/PhysRevE.82.046116 PACS number(s): 82.40.Ck, 89.75.Da, 89.75.Hc, 07.10.Cm

I. INTRODUCTION

Various complex systems consist of different particles, e.g., atoms in chemical materials [1], organisms in ecological systems [2], people in social communities [3], documents in computer networks [4], etc. Typically, particles of same scale locally react with each other and diffuse in space, forming the so-called reaction-diffusion (RD) processes [5], which have been widely studied and used to model spatially distributed dynamics such as chemical reactions [6], population evolution [7], epidemic or computer virus spreading [4,8], and so on. Obviously, the results produced by RD processes, i.e., spatial distributions of different types of particles, are not only determined by the reaction equations but also largely influenced by the topological structures of their underlying networks in which the diffusions take place.

RD processes are usually simulated on regular lattices as a good approximation of the Euclidean space [9,10]. Particles are randomly placed in some lattice nodes and those in the same node react with each other. At the same time, they diffuse to neighboring nodes simultaneously. Traditionally, there are two types of RD processes: fermionic RD processes, such as the diffusion-annihilation [11] and the diffusion-coagulation [12] processes, assuming that there is a limitation on the number of particles in each node, and bosonic RD processes [13,14], such as the classical chemical reactions and the epidemic spreading on metropolitan networks where particles represent people traveling between different locations, allowing each node to be occupied by any finite number of particles. Recently, it was revealed that many real-world biological [15], social [16], and technological [17] systems can be described by networks or graphs and they share a common property of having heterogeneous structures. Various RD processes are now being studied on heterogeneous networks, such as scale-free networks [18,19], characterized by nontrivial power-law degree distributions. It has been found that most RD processes on heterogeneous networks behave totally differently from those on regular lattices [11–14]. These research results are very interesting and seem more realistic and suitable for explaining many observed phenomena.

But, why are there so many real-world networks possessing a similar heterogeneous structure with a power-law degree distribution? Does this structural feature benefit the networks on their dynamics, e.g., RD processes? Although the preferential attachment rule [18] (i.e., a newly added node always prefers to connect to an existent node of larger degree) and its expanding versions, such as hierarchical models [20], ranking models [21], and local-world models [22,23], can indeed explain the power-law degree distribution, such structure-based mechanisms are unable to answer the second question which is more essential. Colizza *et al.* [13] pointed out that heterogeneous networks indeed have advantages in producing more active particles in a susceptible-infected-susceptible model, as further detailed by Baronchelli *et al.* in [14].

In this paper, we investigate a closely related problem as to whether or not, and how, RD processes and environmental conditions can shape the network structure via a local rewiring process. This study may provide a good explanation for the common structural heterogeneity revealed in many real-world networks. More importantly, as a distributed control problem [24], it also provides a new way to dynamically

*Author to whom all the correspondence should be addressed; crestxq@hotmail.com

adjust the equilibrium points of a chemical reaction process so as to increase the conversion rate by slightly changing the structure of the underlying network in the embedded space. It seems especially useful for microfabrication techniques [25,26], which are becoming more and more popular in industry today due to their enormous advantages in green environmental protection, energy conservation, waste reduction, and security operation.

The rest of the paper is organized as follows. In Sec. II, some theoretical analysis is reviewed for a special bosonic RD process on a network. In Sec. III, a framework of structure control is proposed and the corresponding numerical mechanism of an adaptive network is introduced. The structure of the network in different stages is carefully investigated in Sec. IV, and the RD results are analyzed in Sec. V. The work is finally summarized in Sec. VI.

II. THEORETICAL BACKGROUND

In order to investigate the effects of a typical chemical reaction process and its environmental conditions on the underlying network structure, we adopt a simple model with only two types of particles, which has been studied in both physics and mathematical epidemiology [13]. The process is composed of the following two reactions:

$$\beta \rightarrow \alpha, \tag{1}$$

$$\alpha + \beta \rightarrow 2\beta. \tag{2}$$

From these reaction equations, one can see that the total number of particles does not change in the process. Here, β particles are identified as active particles because α particles cannot spontaneously generate β particles. Denoting the reaction rates of Eqs. (1) and (2) by μ_1 and μ_2 and the current numbers of α and β particles in node i by $n_{\alpha,i}(t)$ and $n_{\beta,i}(t)$, respectively, each time, after reaction, the numbers of α and β particles in node i change to

$$\tilde{n}_{\alpha,i}(t) = n_{\alpha,i}(t) + \mu_1 n_{\beta,i}(t) - \mu_2 \Gamma_i(t), \tag{3}$$

$$\tilde{n}_{\beta,i}(t) = (1-\mu_1) n_{\beta,i}(t) + \mu_2 \Gamma_i(t), \tag{4}$$

where the reaction kernel $\Gamma_i(t)$ takes the form of $\Gamma_i(t) = n_{\alpha,i}(t) n_{\beta,i}(t)$. Each time, in diffusion process, a number of particles jump out of node i to its neighbors, at the same time, another group of particles jump into node i from its neighbors, denoting the diffusion rates of two types of particles by η_α and η_β, respectively, then, after RD process, the total numbers of particles in node i can be statistically recalculated by

$$n_{\alpha,i}(t+1) = (1-\eta_\alpha)\tilde{n}_{\alpha,i}(t) + \eta_\alpha \sum_{j \in \pi_i} \frac{\tilde{n}_{\alpha,j}(t)}{k_j}, \tag{5}$$

$$n_{\beta,i}(t+1) = (1-\eta_\beta)\tilde{n}_{\beta,i}(t) + \eta_\beta \sum_{j \in \pi_i} \frac{\tilde{n}_{\beta,j}(t)}{k_j}, \tag{6}$$

where π_i is the neighboring set of node i. From Eqs. (3)–(6), it can be easily concluded that the dynamical RD equations in each node i can be represented by

$$\frac{\partial n_{\alpha,i}}{\partial t} = -n_{\alpha,i} + (1-\eta_\alpha)[\mu_1 n_{\beta,i} + n_{\alpha,i} - \mu_2 \Gamma_i] + \eta_\alpha \left[\sum_{j \in \pi_i} \frac{\mu_1 n_{\beta,j} + n_{\alpha,j} - \mu_2 \Gamma_j}{k_j} \right], \tag{7}$$

$$\frac{\partial n_{\beta,i}}{\partial t} = -n_{\beta,i} + (1-\eta_\beta)[(1-\mu_1) n_{\beta,i} + \mu_2 \Gamma_i] + \eta_\beta \left[\sum_{j \in \pi_i} \frac{(1-\mu_1) n_{\beta,j} + \mu_2 \Gamma_j}{k_j} \right], \tag{8}$$

where the time indices t are dropped for convenience and η_α, η_β, μ_1, and μ_2 are all constants. Supposing $\eta_\alpha = \eta_\beta = \eta$ and denoting the number of total particles in node i by $n_i = n_{\alpha,i} + n_{\beta,i}$, after summing Eqs. (7) and (8), one has

$$\frac{\partial n_i}{\partial t} = \eta \left(\sum_{j \in \pi_i} \frac{n_j}{k_j} - n_i \right). \tag{9}$$

Denoting $\phi_i = n_i / k_i$, Eq. (9) becomes

$$k_i \frac{\partial \phi_i}{\partial t} = \eta \left(\sum_{j \in \pi_i} \phi_j - k_i \phi_i \right). \tag{10}$$

Assume that the RD process takes place on a connected network with totally V nodes, defined by an adjacency matrix A with element a_{ij} equal to 1 if nodes i and j are connected and 0 otherwise. Then, Eq. (10) can be further simplified to a matrix form,

$$\frac{\partial \phi}{\partial t} = \eta K^{-1} L \phi, \tag{11}$$

where $\phi = [\phi_1, \phi_2, \ldots, \phi_V]^T$, $K = \mathrm{diag}(k_1, k_2, \ldots, k_V)$, and $L = A - K$ is the well-known Laplacian matrix. Equation (11) has a steady solution $\phi = [c, c, \ldots, c]^T$ under the condition $\sum_{i=1}^{V} n_i = \sum_{i=1}^{V} k_i \phi_i = cV\langle k \rangle = N$, where $N = \sum_{i=1}^{V} n_i$ is the total number of particles on the network. Denoting $\rho = N/V$, one has $c = \rho / \langle k \rangle$, so that the steady solution of Eq. (9) can be obtained as

$$n_i = \frac{k_i}{\langle k \rangle} \rho. \tag{12}$$

This result is consistent with the solution derived by the mean-field theory [13,14,27] when considering only the diffusion process of a single type of bosonic particles on a network, which means that a node of larger degree always attracts more particles to pass through it.

Suppose there are V_k nodes possessing degree k in the network and denoting by $N_{\alpha,k}$ and $N_{\beta,k}$ the numbers of α and β particles, respectively, in these nodes. Then, the quantities

$$\rho_{\alpha,k} = \frac{N_{\alpha,k}}{V_k}, \quad \rho_{\beta,k} = \frac{N_{\beta,k}}{V_k} \tag{13}$$

represent the average numbers of α and β particles, respectively, in each node of degree k, denoting by $P(k)$ the degree distribution of the network. Then, by the mean-field theory and under the assumption of no degree correlation between linked nodes [13], Eqs. (7) and (8) become

$$\frac{\partial \rho_{\alpha,k}}{\partial t} = -\rho_{\alpha,k} + (1-\eta_\alpha)[\mu_1 \rho_{\beta,k} + \rho_{\alpha,k} - \mu_2 \Omega_k] + \frac{\eta_\alpha k}{\langle k \rangle}[\mu_1 \rho_\beta + \rho_\alpha - \mu_2 \Omega], \tag{14}$$

$$\frac{\partial \rho_{\beta,k}}{\partial t} = -\rho_{\beta,k} + (1-\eta_\beta)[(1-\mu_1)\rho_{\beta,k} + \mu_2 \Omega_k] + \frac{\eta_\beta k}{\langle k \rangle}[(1-\mu_1)\rho_\beta + \mu_2 \Omega], \tag{15}$$

with $\rho_\alpha = \Sigma_k P(k)\rho_{\alpha,k}$, $\rho_\beta = \Sigma_k P(k)\rho_{\beta,k}$, and $\Omega = \Sigma_k P(k)\Omega_k$, where the reaction kernel now takes the form of $\Omega_k = \rho_{\alpha,k}\rho_{\beta,k}$.

Let $\eta_\alpha = \eta_\beta = 1$ throughout the paper. Equations (14) and (15) have simple steady solutions,

$$\rho_{\alpha,k} = \frac{k}{\langle k \rangle}\rho_\alpha, \quad \rho_{\beta,k} = \frac{k}{\langle k \rangle}\rho_\beta, \tag{16}$$

with

$$\rho_\alpha = \rho - \frac{\mu_2}{\mu_1}\Omega, \quad \rho_\beta = \frac{\mu_2}{\mu_1}\Omega. \tag{17}$$

From Eqs. (16) and (17) and the definition of Ω, one can get the average densities of α and β particles, respectively, on the network

$$\rho_\alpha = \frac{\mu_1}{\mu_2}\frac{\langle k \rangle^2}{\langle k^2 \rangle}, \quad \rho_\beta = \rho - \frac{\mu_1}{\mu_2}\frac{\langle k \rangle^2}{\langle k^2 \rangle}, \tag{18}$$

when the dynamics is statistically steady. In Eq. (18), one can see that the steady-state density of β particles on the network is indeed not only determined by the reaction parameters, such as ρ, μ_1, and μ_2, but also influenced by a degree-related structural property of the network, $\langle k \rangle^2/\langle k^2 \rangle$, the value of which is typically used to define the heterogeneity of a network, i.e.,

$$H = \frac{\langle k^2 \rangle}{\langle k \rangle^2}. \tag{19}$$

III. MECHANISM

Now, we propose a feedback framework to study the emergence of the heterogeneous structure when each node in the network has the ability to sense the environment and to rearrange its neighbors.

In many cases, nodes in a network are considered as different kinds of agents [28,29], which can rearrange their associates in a planed or random way in order to increase their advantages in natural or social competitions. For RD processes, such advantages may be reflected by certain ratios of particles in the nodes, e.g., $n_{\beta,i}/n_i$. Motivated by these observations, we propose a feedback framework as shown in Fig. 1. Intuitively, different external conditions may lead to adaptive networks of different topological structures. In this paper, specially, the network dynamics are performed by the following five steps:

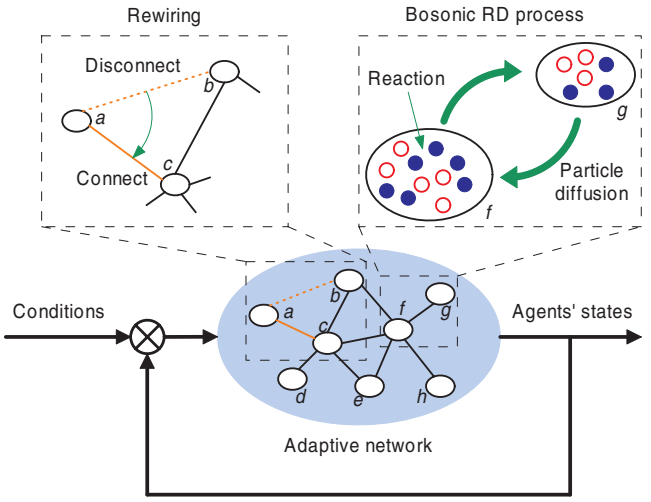

FIG. 1. (Color online) The RD-driven adaptive network. Here, only the bosonic RD process is considered. α and β particles diffuse on the network but inside each node they react with each other. Each node can sense the environment, and once the ratio of α or β in a node does not meet the external natural or artificial conditions or requirements, the node undergoes a rewiring process, and thus the network evolves adaptively as the external conditions change.

(1) *Initialization.* To start, numbers $N_\alpha(0)$ of α particles and $N_\beta(0)$ of β particles are randomly distributed in an $L \times L$ two-dimensional lattice containing $V = L^2$ nodes. Set $\gamma = 0$.

(2) *Reaction.* At every time step t, in each node i, numbers $n_{\alpha,i}(t-1)$ of α particles and $n_{\beta,i}(t-1)$ of β particles react with each other according to Eqs. (1) and (2). Here, $n_{\alpha,i}(t-1)$ and $n_{\beta,i}(t-1)$ can be any integers including zero. That is, with probability μ_1, particle β is transformed to particle α, and at the same time, with probability $1-(1-\mu_2)^{n_{\beta,i}(t-1)}$, particle α is transformed to particle β [13].

(3) *Diffusion.* After every reaction, all the particles in each node diffuse to its direct neighbors with an equal probability; i.e., at each time step, a particle in a node with degree k will jump into one of its direct neighbors with probability $1/k$. Then, the number of α particles and that of β particles in each node i are updated by $n_{\alpha,i}(t)$ and $n_{\beta,i}(t)$, respectively.

(4) *Rewiring.* When $t > T_s$ (T_s is a sufficient number of time steps needed to achieve a relatively steady state), in every τ ($\tau \gg 1$) time steps, count the total times τ_i^f that the state of each node i fails to meet the external conditions. Once $\tau_i^f/\tau > \xi$, node i is added into a rewiring candidate set R. If $R = \varnothing$, set $\gamma = \gamma + 1$; otherwise, randomly select a candidate from the set R, denoted by a, and one of its neighbors, denoted by b, release the link between them, and then create a new link between node a and one neighbor of node b, denoted by c, as shown in Fig. 1. It should be noted that self-loops and multiple edges are not allowed; therefore, if node a and node c were already connected, then the network keeps unchanged and the rewiring is canceled. Set $R = \varnothing$, $\gamma = 0$, and turn to step 2. Such a local rewiring strategy is quite natural, which does not change the total connectivity of the network. For each node i, the external condition or requirement could be to encourage or to discourage the active particles β, as represented by

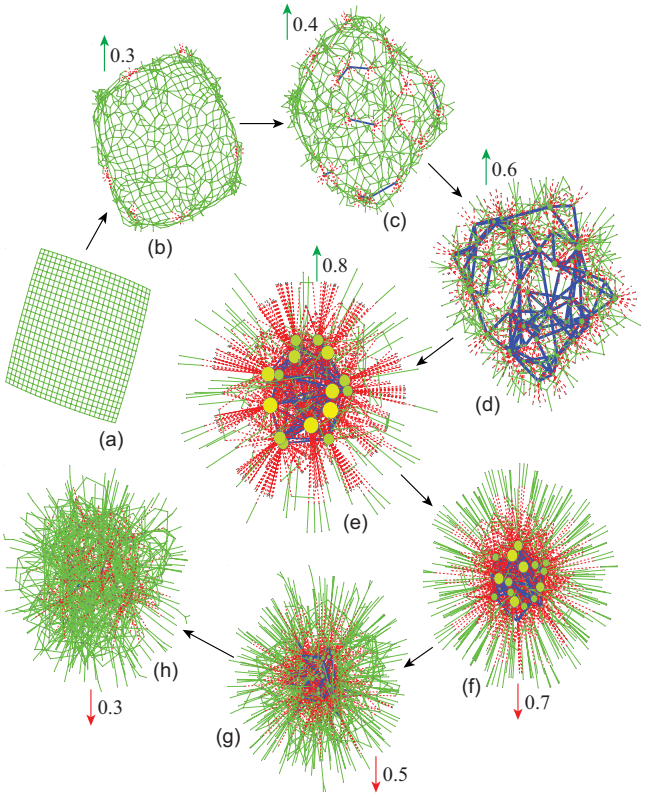

FIG. 2. (Color online) (a) The initial lattice as well as some scenes of the adaptive network in different stages: (b)–(e) increasing stages $\theta=0.3$, 0.4, 0.6, and 0.8; (f)–(h) decreasing stages $\theta=0.7$, 0.5, and 0.3. The node size is proportional to the node degree. In each scene, the links between the nodes with degree not smaller than 10 are plotted by blue bold lines, those between the nodes with degree smaller than 10 are plotted by green solid lines, and the remaining ones (the links between high-degree nodes and low-degree nodes) are plotted by red dashed lines.

$$\sigma_{\beta,i}=\frac{n_{\beta,i}}{n_i}>\theta, \tag{20}$$

$$\sigma_{\beta,i}=\frac{n_{\beta,i}}{n_i}<\theta. \tag{21}$$

(5) *Termination*. When $\gamma=T_1$ or $t=T_2$, the process is terminated.

When the size of the lattice and the number of particles are fixed, the parameter θ in Eqs. (20) and (21) is the only input to the system which determines the final RD steady states and the structure of the adaptive network. In simulation, we steadily increase θ from 0.1 to 0.8 adopting the condition of Eq. (20) and then decrease it from 0.8 to 0.1 adopting the different condition of Eq. (21), so as to study the responses of the adaptive network. When the parameters are set to be $\mu_1=0.2$, $\mu_2=0.05$, $\rho=5$ with $\rho_\alpha(0)/\rho_\beta(0)=N_\alpha(0)/N_\beta(0)=1$, $V=L^2=625$, $\xi=0.9$, $T_s=10^6$, $\tau=100$, $T_1=200$, and $T_2=10^7$, the scenes of the adaptive network in different stages are shown in Fig. 2. Note that, with the values chosen for the reaction rates, the proportion of α or β particles in the whole network can change steadily in a large range as the network evolves. With the values chosen for the parameters ξ, τ, and T_1, in most cases, the structure of the network is changed frequently at the beginning and can be statistically stable at somewhere in limited steps when a new environmental condition is provided.

Intuitively, in the increasing stages by adopting the condition of Eq. (20), the adaptive network is getting more and more heterogeneous so that most of nodes in the network can possess relatively higher ratios of active particles β. At the beginning, high-degree nodes (e.g., $k\geq 10$) emerge separately, as shown in Fig. 2(c). As the requirement is further enhanced, these hub nodes begin to connect with each other and a prominent skeleton, i.e., the subnetwork connected by the blue bold lines in Fig. 2(d), comes into being. The skeleton is further condensed when θ increases to 0.8 and, in this stage, a kernel forms and the adaptive network evolves to a quasistar network, as shown in Fig. 2(e). In the opposite direction by adopting the condition of Eq. (21), the kernel explodes until most of the hub nodes disappear and the network becomes homogeneous again.

IV. STRUCTURAL PROPERTIES

In the past decade, more and more countermeasures [30], such as degree, clustering coefficient, distance, assortativity [31], symmetry [32], and so on, have been proposed. Such measures, whether they originated from practical engineering problems or are just mathematically inspired, provide a way to quantitatively compare and further classify and model different real-world complex networks.

Essentially, the adaptive network proposed in this paper provides a set of network scenes through its continuously adjusting the structure to satisfy the external conditions. Characterizing this adaptive network in different stages has scientific significance because the obtained structural properties may validate the structural similarity between the adaptive network in some stages and those real-world biological or technological networks. More importantly, in this case we can say that the common heterogeneous structure of these networks is a natural result of adaptation. Hopefully, it can help engineers to design better reconstructing mechanisms for technological networks, such as microreactor networks and data-traffic networks, to produce more required or less unwilling particles as quickly as possible in RD processes.

Next, we review several classical network measures and then adopt them to characterize the proposed adaptive network in different stages. The first one is the heterogeneity defined by Eq. (19). In the literature, heterogeneous networks are usually depreciated due to their weakness to hub-node attacks [33], unbalanced load distribution [34], and poor synchronizing ability [35], although these types of networks are quite universal in the real world. Here, as can be seen in Fig. 3(a), the adaptive network indeed gets more heterogeneous spontaneously when each node can only sense the environmental conditions for more active particles and to rearrange their neighbors independently. Perhaps this is one reason why heterogeneous structure is still widely encountered in biological and technological systems although it may be undesirable for some other dynamics.

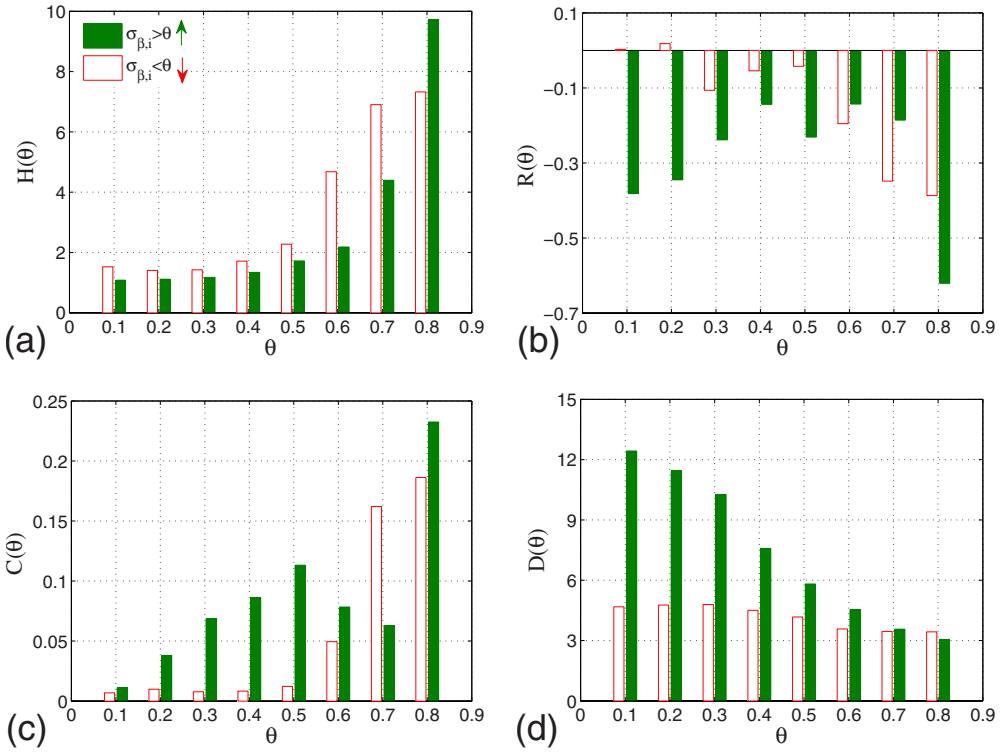

FIG. 3. (Color online) Several topological properties, such as (a) heterogeneity, (b) average assortativity coefficient, (c) average clustering coefficient, and (d) average distance for the adaptive network in different increasing and decreasing stages.

In a network, it is also very interesting to investigate whether high-degree nodes prefer to attach to other high-degree nodes (assortativeness) or to low-degree ones (disassortativeness). In order to measure such preference more quantitatively, Newman [31] proposed a normalized assortativity coefficient, $-1 \le R \le 1$, represented by

$$R = \frac{M^{-1}\sum_j p_j q_j - \left[M^{-1}\sum_j \frac{1}{2}(p_j + q_j)\right]^2}{M^{-1}\sum_j \frac{1}{2}(p_j^2 + q_j^2) - \left[M^{-1}\sum_j \frac{1}{2}(p_j + q_j)\right]^2}, \quad (22)$$

where p_j and q_j are the degrees of the end nodes of the jth link, with $j=1,\ldots,M$. Newman [31] found that social networks are mostly assortative ($R>0$), while biological and technological networks are mostly disassortative ($R<0$), and some artificial networks are nonassortative ($R\approx 0$). Generally, the adaptive network proposed here is disassortative in most evolving stages, as shown in Fig. 3(b). Such disassortativity is slightly weakened as θ increases in the increasing stages before the network evolves to possessing a quasistar structure. In this process, more and more large-degree nodes emerge and they are connected with each other to form a skeleton of the adaptive network, as shown in Fig. 2(d). Such a structure may improve the transferring efficiency of particles and further help produce more active particles. In the decreasing stages, the adaptive network becomes more and more homogeneous as θ decreases, and it seems quite natural that the disassortativity also steadily weakens in this process. It should be noted that such a degree correlation is obviously inconsistent with the above no-correlation assumption when we attempt to infer the theoretical solutions of Eqs. (7) and (8) by the mean-field theory. As a result, there could be a gap between theoretical and experimental results, which will be further discussed in Sec. V.

The clustering coefficient of node i, representing the connecting density among its neighbors, is denoted by

$$C_i = \frac{2e_i}{|\pi_i|(|\pi_i|-1)}, \quad (23)$$

where e_i is the total number of links among its $|\pi_i|$ neighbors. The network distance between two nodes is defined by the smallest number of connections included in any path between them. Moreover, the average clustering coefficient C and the average distance D are always considered together in the literature [36] to investigate whether the studied network is both highly clustering (large C) and small world (small D), like many real-world networks. For the adaptive network, these properties could be achieved in the increasing stages when θ is large enough, i.e., $\theta \ge 0.6$, as shown in Figs. 3(c) and 3(d). It should be noted that the requirement $\sigma_{B,i} > 0.8$ seems much too strict. In fact, the adaptive network cannot satisfy such a requirement when other parameters keep unchanged. The adaptive dynamics are forcibly terminated by the condition $T=10^7$ and, naturally, the quasistar structure shown in Fig. 2(e) is unreachable.

As one can see, all these characteristics, namely, heterogeneous, disassortative, highly clustering, and small-world features, can be reproduced in this adaptive network when $\theta \ge 0.6$. In order to provide more structural evidences, we

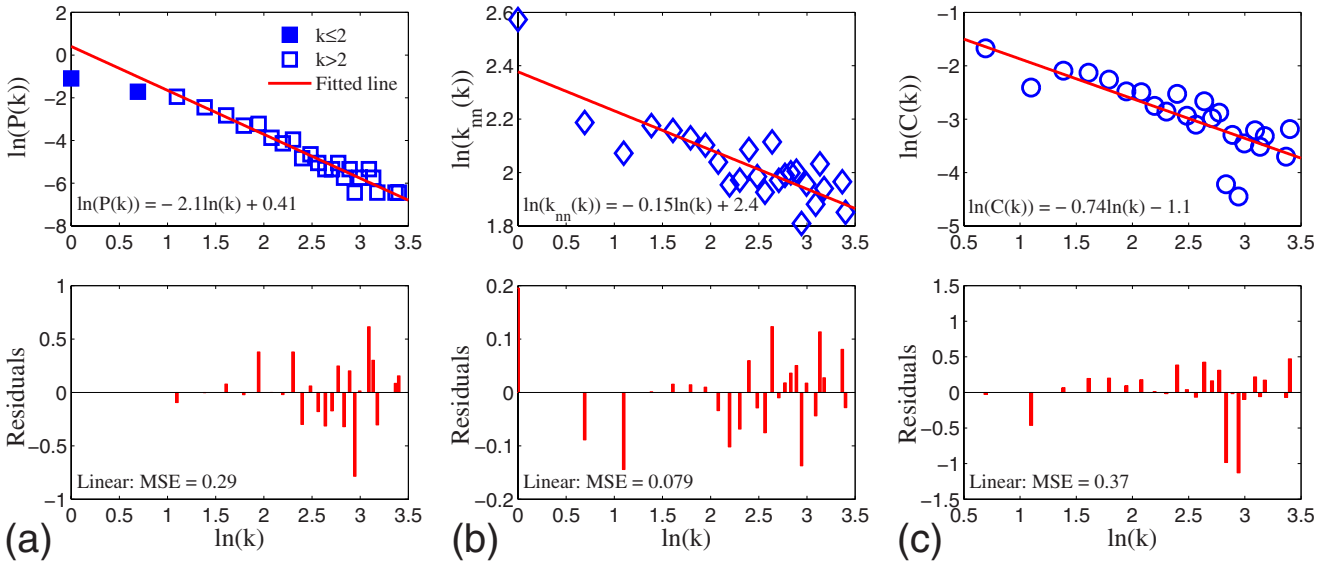

FIG. 4. (Color online) (a) Degree distribution, (b) degree correlation function, and (c) clustering function as well as their fitted lines and linear residuals for the stable adaptive network scene in the increasing stage when $\theta=0.6$.

also investigated several other topological properties of the adaptive network in the increasing stage when $\theta=0.6$. Although the relatively small maximum node degree makes it somewhat ambiguous to claim that some distribution related to degree k follows a certain distribution form, its degree distribution $P(k)$ representing the fraction of nodes with degree k indeed seems compatible with the scale-free property, i.e., $P(k)\sim k^{-\lambda_1}$ with $\lambda_1=2.1$. This is consistent with the reports on many other real-world complex networks [16–18,37]. Besides, its degree correlation function $k_{nn}(k)$, denoting the average degree on the nodes directly connected to those with degree k, and its clustering function $C(k)$, denoting the average clustering coefficient on the nodes with degree k (Fig. 4), are also compatible with the scale-free property, i.e., $k_{nn}(k)\sim k^{-\lambda_2}$ and $C(k)\sim k^{-\lambda_3}$ with $\lambda_2=0.15$ and $\lambda_3=0.74$ (close to 1), respectively, both frequently seen in technological and biological networks [31,38,39].

All of these phenomena suggest that many real-world networks as self-organized systems may experience inner RD dynamics. In order to increase the proportion of certain particles to satisfy the environmental conditions, each node in such a network undergoes a rewiring process, so finally a similar heterogeneous structure emerges. Such an explanation sounds more substantial than the argument based only on topological rules. More interestingly, when the external conditions discourage the active particles, the adaptive network evolves to a relatively homogeneous structure with lower clustering and a smaller average distance instead. It has been revealed [40] that such a structure has its advantage in some other aspects, such as being robust to attacks, balancing load distribution, and synchronizing individuals' dynamics.

V. RD PROCESS

Assume that each node i in the adaptive network as an agent can sense the difference between its state $\sigma_{B,i}$ and the external conditions specified by Eq. (20) or (21) and at the same time has the ability to respond to the difference by rearranging its neighbors. Through a local randomly rewiring process as described in Fig. 1, it appears that most nodes can independently find their right places in the network to statistically decrease or even eliminate the differences between their states and those not so strict conditions, and finally the adaptive network can be stabilized onto somewhere and the RD equilibrium can be reached.

Next, we investigate the corresponding shift of the RD equilibrium and the proportions of different reactants in the adaptive network under different environmental conditions. Given the total density of particles ρ and the reaction parameters μ_1 and μ_2, it was proven [13] that the RD result is determined only by the network structure and is independent of the initial ratio $\rho_\alpha(0)/\rho_\beta(0)$, except for very early time transients. Here, we study the RD process in different adaptive network scenes obtained by the mechanism introduced in Sec. II under different external conditions. The average ratio of β particles over all the nodes and the proportion of β particles in the whole network are defined by

$$\sigma_\beta=\frac{1}{V}\sum_{i=1}^{V}\sigma_{\beta,i}, \tag{24}$$

$$\chi_\beta=\frac{\rho_\beta}{\rho}, \tag{25}$$

respectively. Generally, both σ_β and χ_β increase steadily as the threshold θ is increased in the increasing stages when β particles are encouraged and decrease when β particles are discouraged, as shown in Figs. 5(a) and 5(b). This phenomenon suggests that the RD equilibrium in each node, and furthermore that in the whole network, can indeed be statistically controlled by a local rewiring process. This is especially important for biological networks where each component may not have information about the structure of the

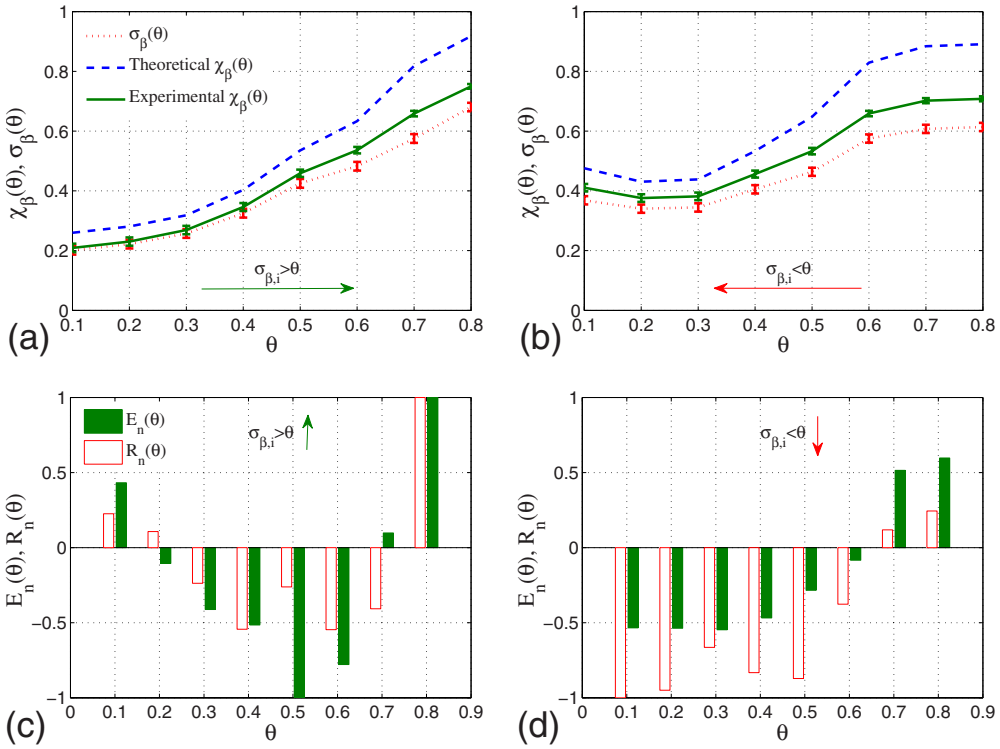

FIG. 5. (Color online) The average ratio of β particles over all the nodes and the theoretical and experimental proportions of β particles in the whole network in the adaptive network: (a) increasing stages; (b) decreasing stages. The normalized error between the theoretical and experimental proportions of β particles and the normalized average assortativity coefficient of the network: (c) increasing stages; (d) decreasing stages. In each network scene, the RD process is parallelly implemented for 10^4 times after the early time transients and then the corresponding results are recorded.

whole network and the inner reaction rates cannot be adjusted by changing some macroscopic measures such as temperature, pressure, and so on.

Moreover, from Eqs. (18), (19), and (25), one can get the theoretical average proportion of β particles in the whole network as follows:

$$\chi_\beta = 1 - \frac{\mu_1}{\rho\mu_2}\frac{1}{H}. \tag{26}$$

When the parameters are set to be $\rho=5$, $\mu_1=0.2$, and $\mu_2=0.05$, Eq. (26) can be simplified to be $\chi_\beta=1-0.8/H$. Theoretical χ_β in different stages is also shown in Figs. 5(a) and 5(b) by dashed lines. As mentioned, the distinct gap between theoretical and experimental χ_β may be caused by the definite degree correlation between pairwise linked nodes in the adaptive network because the theoretical result is obtained by the mean-field theory under the assumption of having no such degree correlations. Denoting by $E(\theta)$ the difference between theoretical and experimental χ_β for a certain θ in the increasing or decreasing stage and by E_{min} and E_{max} the corresponding minimum and maximum values, respectively, the difference can be normalized in $[-1,1]$ by

$$E_n(\theta) = \frac{2}{E_{max}-E_{min}}[E(\theta)-E_{min}] - 1. \tag{27}$$

Similarly, the absolute value of the assortativity coefficient of the adaptive network at certain θ can be normalized in $[-1,1]$ by

$$R_n(\theta) = \frac{2}{|R|_{max}-|R|_{min}}[|R(\theta)|-|R|_{min}] - 1. \tag{28}$$

The values of $E_n(\theta)$ and $R_n(\theta)$ in different increasing and decreasing stages are shown in Figs. 5(c) and 5(d), respectively, where one can see that $E_n(\theta)$ and $R_n(\theta)$ are indeed strongly correlated with each other in most cases; i.e., $E_n(\theta)\times R_n(\theta)>0$ is satisfied. In other words, the mean-field theory may fail to produce an acceptable result if there is a strong degree correlation between pairwise linked nodes in the adaptive network.

When both α and β particles are allowed to diffuse, it is quite natural that nodes of larger degrees always contain more particles [13]. As predicted by Eqs. (12) and (16), one has $\rho_{\alpha,k}=\varsigma_\alpha k+\delta_\alpha$ and $\rho_{\beta,k}=\varsigma_\beta k+\delta_\beta$, where the parameters can be calculated as $\varsigma_\alpha=\rho_\alpha/\langle k\rangle=1.7068/3.84=0.44$ and $\varsigma_\beta=\rho_\beta/\langle k\rangle=3.2932/3.84=0.86$ in the increasing stage when $\theta=0.7$. This can also be validated by the simulations shown in Fig. 6(a). Moreover, in Fig. 6(b), one can see that the average ratio of β particles inside nodes of degree k, denoted by $\sigma_\beta(k)$, keeps almost constant as $k>1$ increases. This is the reason why the adaptive network can be statistically stabilized onto somewhere when each node is exposed to the same external conditions specified by Eqs. (20) and (21). The somewhat smaller value of $\sigma_\beta(1)\approx 0.5$ may be caused by the low density of particles in the leaf nodes of degree 1. In fact, there are always no β particles in these nodes when the av-

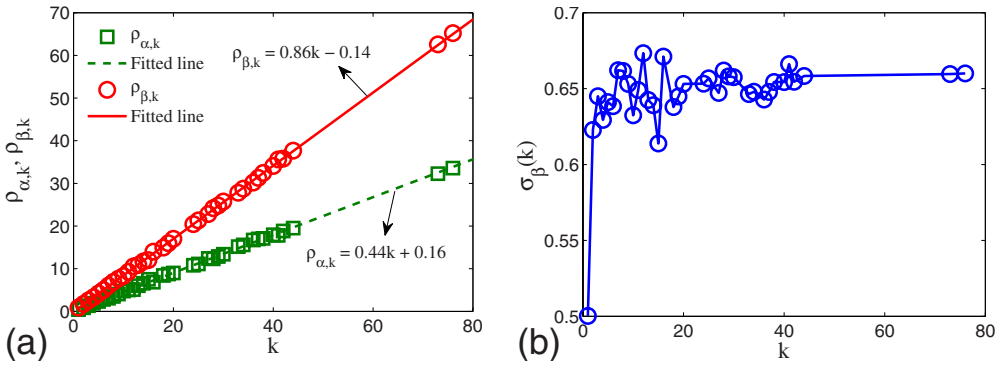

FIG. 6. (Color online) (a) Average densities of α particles and β particles inside nodes of degree k as linear functions of k in the increasing stage when θ=0.7. (b) Average ratio of β particles inside nodes of degree k keeps almost constant for various values of k.

erage density of β particles is close to $\varsigma_\beta/(\varsigma_\alpha+\varsigma_\beta)=0.72$, as shown in the above simulation figures.

VI. SUMMARY

The mechanism introduced here can be used to study the effects of microscopic reaction-diffusion processes on the structures of the underlying networks, which can provide more convincing explanations for the existence of common heterogeneous structures of many biological and technological networks. Furthermore, the approach may provide a way for engineers to design changeable reactor networks where chemical equilibriums can be dynamically adjusted by a simple reactor rewiring process, which is especially useful in the area of microfabrication industries. In the future, more chemical reaction-diffusion processes will be considered under the new framework and better structural control strategies will be developed.

ACKNOWLEDGMENTS

We would like to thank all the members in the Center for Chaos and Complex Networks in the City University of Hong Kong for their valuable discussions about the ideas and some technical details presented in this paper. The work was supported by the National Natural Science Foundation of China Grant No. 61004097 and the NSFC-HKRGC Joint Research Scheme Grant No. CityU_N107/07.

[1] J. C. Meyer, C. O. Girit, M. F. Crommie, and A. Zettl, Nature (London) **454**, 319 (2008).
[2] J. Y. Wakano, M. A. Nowak, and C. Hauert, Proc. Natl. Acad. Sci. U.S.A. **106**, 7910 (2009).
[3] C. Cattuto, A. Barrat, A. Baldassarri, G. Schehr, and V. Loreto, Proc. Natl. Acad. Sci. U.S.A. **106**, 10511 (2009).
[4] P. Wang, M. C. González, C. A. Hidalgo, and A.-L. Barabási, Science **324**, 1071 (2009).
[5] A. M. Turing, Philos. Trans. R. Soc. London, Ser. B **237**, 37 (1952).
[6] B. A. Grzybowski, *Chemistry in Motion: Reaction-Diffusion Systems for Micro- and Nanotechnology* (Wiley, Chichester, West Sussex, 2009).
[7] R. S. Cantrell and C. Cosner, *Spatial Ecology via Reaction-Diffusion Equations* (Wiley, Chichester, West Sussex, 2003).
[8] V. Colizza, A. Barrat, M. Barthélemy, and A. Vespignani, Proc. Natl. Acad. Sci. U.S.A. **103**, 2015 (2006).
[9] D. Dab, J.-P. Boon, and Y.-X. Li, Phys. Rev. Lett. **66**, 2535 (1991).
[10] J. P. Boon, D. Dab, R. Kapral, and A. Lawniczak, Phys. Rep. **273**, 55 (1996).
[11] L. K. Gallos and P. Argyrakis, Phys. Rev. Lett. **92**, 138301 (2004).
[12] S. Weber and M. Porto, Phys. Rev. E **74**, 046108 (2006).
[13] V. Colizza R. Pastor-Satorras, and A. Vespignani, Nat. Phys. **3**, 276 (2007).
[14] A. Baronchelli, M. Catanzaro, and R. Pastor-Satorras, Phys. Rev. E **78**, 016111 (2008).
[15] A.-L. Barabási and Z. N. Oltvai, Nat. Rev. Genet. **5**, 101 (2004).
[16] Q. Xuan, F. Du, and T.-J. Wu, Chaos **19**, 023101 (2009).
[17] Z.-Q. Jiang, W.-X. Zhou, B. Xu, and W.-K. Yuan, AIChE J. **53**, 423 (2007).
[18] A.-L. Barabási and R. Albert, Science **286**, 509 (1999).
[19] R. Albert and A.-L. Barabási, Rev. Mod. Phys. **74**, 47 (2002).
[20] Q. Xuan, Y. Li, and T.-J. Wu, Phys. Rev. E **73**, 036105 (2006).
[21] S. Fortunato, A. Flammini, and F. Menczer, Phys. Rev. Lett. **96**, 218701 (2006).
[22] X. Li and G. Chen, Physica A **328**, 274 (2003).
[23] Q. Xuan, Y. Li, and T.-J. Wu, Physica A **378**, 561 (2007).
[24] G. E. Dullerud and R. D'Andrea, IEEE Trans. Autom. Control **49**, 2113 (2004).
[25] W. Ehrfeld, V. Hessel, and H. Löwe, *Microreactors: New Technology for Modern Chemistry* (Wiley, Chichester, West Sussex, 2000).
[26] K. F. Jensen, Chem. Eng. Sci. **56**, 293 (2001).
[27] S. N. Dorogovtsev, A. V. Goltsev, and J. F. F. Mendes, Rev. Mod. Phys. **80**, 1275 (2008).
[28] R. Olfati-Saber, IEEE Trans. Autom. Control **51**, 401 (2006).
[29] Q. Xuan, Y.-J. Li, and T.-J. Wu, Chin. Phys. Lett. **25**, 363

(2008).
[30] L. D. A. F. Costa, F. A. Rodrigues, G. Travieso, and P. R. V. Boas, Adv. Phys. **56**, 167 (2007).
[31] M. E. J. Newman, Phys. Rev. Lett. **89**, 208701 (2002).
[32] Y. Xiao, M. Xiong, W. Wang, and H. Wang, Phys. Rev. E **77**, 066108 (2008).
[33] R. Albert, H. Jeong, and A.-L. Barabási, Nature (London) **406**, 378 (2000).
[34] K.-I. Goh, B. Kahng, and D. Kim, Phys. Rev. Lett. **87**, 278701 (2001).
[35] T. Nishikawa, A. E. Motter, Y.-C. Lai, and F. C. Hoppensteadt, Phys. Rev. Lett. **91**, 014101 (2003).
[36] D. J. Watts and S. H. Strogatz, Nature (London) **393**, 440 (1998).
[37] H. Jeong, B. Tombor, R. Albert, Z. N. Oltvai, and A.-L. Barabási, Nature (London) **407**, 651 (2000).
[38] E. Ravasz, A. L. Somera, D. A. Mongru, Z. N. Oltvai, and A.-L. Barabási, Science **297**, 1551 (2002).
[39] A. Vázquez, R. Pastor-Satorras, and A. Vespignani, Phys. Rev. E **65**, 066130 (2002).
[40] Q. Xuan, Y. Li, and T.-J. Wu, Physica A **388**, 1257 (2009).